Electrospun Asymmetric Membranes

Subjects: Others

Contributor: Ilídio Correia

Asymmetric electrospun membranes are 3D matrices composed of two layers with different nanofiber-based structures, reproducing skin's extracellular matrix structure. The external denser layer is often composed of smaller-sized hydrophobic nanofibers, which allows the protection of the wound site against microorganisms invasion. On the other hand, the bottom layer presents a porous interconnected 3D network with hydrophilic nanofibers that promotes a moist environment, which supports cell migration, adhesion, and proliferation. In this way, asymmetric electrospun membranes are able to mimic both epidermis and dermis layers of the skin, through the deposition of one layer on the top of an already produced layer.

asymmetric membranes | bioactive molecules | electrospun membranes | skin regeneration | wound dressing

1. Introduction

Skin is the largest and outermost organ of the human body, with approximately 2 m^2 of area and a mean thickness of 2.5 mm [1][2]. This organ is involved in important functions in the human body, namely thermoregulation, prevention of water and fluid loss, immune surveillance, hormone synthesis, and sensory detection [1][3]. In addition, due to its anatomical location, it also acts as a barrier against microbial invasion as well as mechanical and chemical insults, thus conferring protection to the body [3]. In this way, when the skin's structure is compromised, the use of dressing materials to cover and protect the wound to re-establish a temporary or, in the case of extensive wounds, a permanent fully functional body barrier is of utmost importance [4].

In this field, various biomedical alternatives have been developed and applied over the years to assist the wound healing process. The skin grafts (autografts, allografts, xenografts) remain as the most conventional and widely used therapeutic approach for restoring the skin's structure after an extensive lesion [5]. Despite their intrinsic advantages, autografts present limited availability and induce additional morbidity to the patient; while alo- and xenografts can lead to immune rejection [6][7]. In turn, wound dressings, i.e., 3-dimensional materials/structures that can be applied in the wound site either temporarily or permanently, act as a barrier against microorganisms, external insults, and dehydration, while simultaneously accelerating the wound healing [3][8]. Today, some wound dressings are already applied in the clinic, for example, Duoderm® [9], Acticoat™ [10], Aquacel Ag® [11], DermFactor® [12], and Procellera® [13]. Despite the advantages presented by these commercial wound dressings, they still present drawbacks such as adhesion to the surface of the lesion, which may cause additional damage upon periodic replacement, and the cost [8].

To address these limitations, tissue engineering researchers have been focusing on the development of new different biomimetic wound dressings. Films, hydrogels, and hydrocolloids are some examples, and they present a few advantages such as the capacity to enable the transmission of gases and maintain a moist environment at the wound site, which improves and accelerates the wound healing process [14]. However, these approaches also have some limitations, the possibility of maceration, and the necessity for periodic replacement, and until now, none of them have been capable of fully restoring the skin's native structure and functions [15][16]. Such emphasizes the need for the development of an efficient wound dressing that can provide the ideal structural and biochemical mechanisms for promoting efficient skin regeneration. Asymmetric membranes, widely explored for filtration and gas separation, recently captured the attention of researchers for being applied as wound dressings [17][18][19]. The utilization of asymmetric wound dressings aims to reproduce a skin-like layered organization, which consists in a top layer to protect the wound site and mechanical support, and a bottom layer that facilitates cell migration, adhesion, and proliferation, and provides a moist environment [20]. Particularly, the nanofibrous composition of asymmetric electrospun membranes allows them to reproduce the extracellular matrix (ECM) structure, thus providing additional anchoring points for cell adhesion and proliferation [21].

2. Electrospun Asymmetric Membranes as Delivery Systems of Biomolecules

Apart from the structural advantages of asymmetric electrospun membranes, the nanofibers present in their structure can also incorporate bioactive agents for increasing its antibacterial efficacy and/or enhance the wound healing process (Figure 4). Table 3 provides an overview of the biologic properties of asymmetric membranes produced through electrospinning aimed to be used as wound dressings.

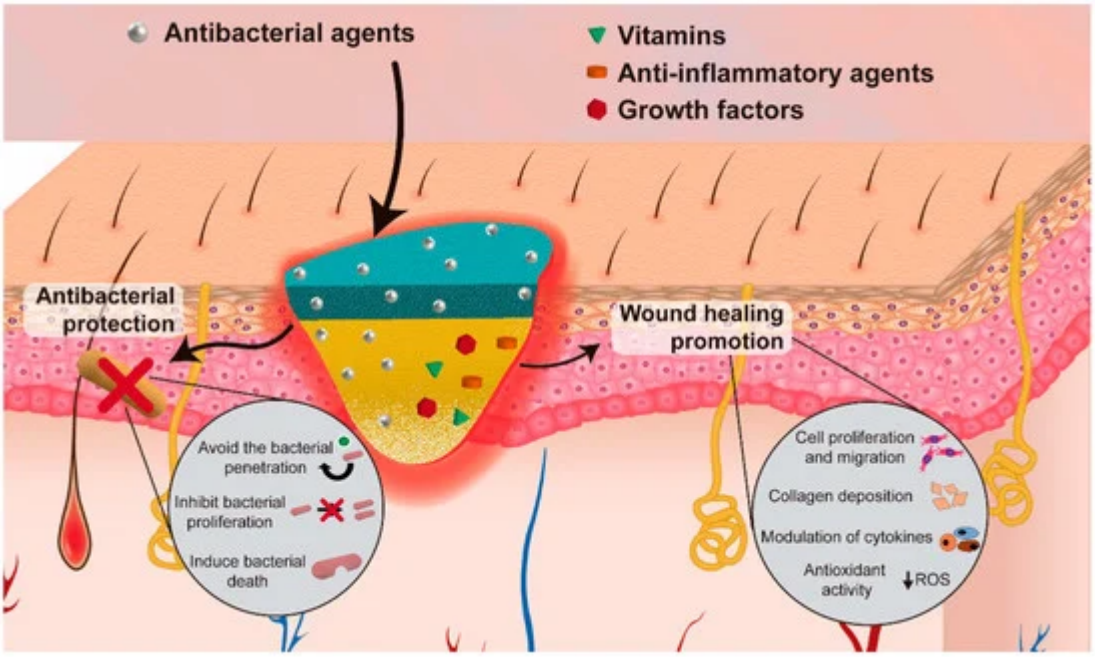

Figure 4. Illustration of the incorporation of bioactive agents to improve the antibacterial efficacy and/or enhance the wound healing process.

Table 3. Asymmetric membranes produced through electrospinning aimed to be used as biomolecules delivery systems.

Aims	Composition	Biomolecule Incorporated	Layer of Incorporation	Encapsulation Efficiency and Loading Efficiency	Release Profile	Ref
Antibacterial activity	PCL/PVAc	CRV	Bottom layer	The CRV loaded in samples I and II was 3.0 ± 0.4 wt% and 2.3 ± 0.5 wt%, respectively	Sample I released about 45% of the total drug, while sample II released about 60% of the loaded CRV, at pH 8; after 7 days in basic pH the membranes were transferred to PBS pH 7.4 and after two weeks in this medium the release reached 60% and 85% of the loaded drug for samples I and II, respectively; after 14 days, the samples were put in an acidic medium where after one week the release reached 85% and 100% from the samples I and II, respectively	[22]
	(Sample I—PVAc in DMF/ETOH; sample II—PVAc in DMF)			Encapsulation efficiencies were 55 ± 5% and 43 ± 9% for samples I and II, respectively		
	PCL-HA/CS-ZN	SA	Bottom layer	N.A.	The release profile, in PBS (pH 5.5), consisted of a burst release in the first hour followed by a sustained release for 5 days (reaching approximately 16%)	[23]
	PCL/PEO-CS	AV	Bottom layer	N.A.	N.A.	[24]
	PCL-SF/SF-HA	THY	Bottom layer	Encapsulation efficiency of 79.7 ± 7.19%	THY release from the nanofibers, at both pH levels, comprises a burst release in the first 8 h after immersion in PBS, followed by a gradual release up to 24 h	[20]

Aims	Composition	Biomolecule Incorporated	Layer of Incorporation	Encapsulation Efficiency and Loading Efficiency	Release Profile	Ref
				Loading efficiency of 64.8 ± 5.42%	At pH 8, the release of THY reached a maximum of 91.87 ± 0.99%	
					At pH 5, the release of THY reached a maximum of 71.75 ± 2.06%	
	PeCL/PDO	TiO_2 nanoparticles (concentration of 3% (PP3T5T) and 5% (PP5T5T)) and TTC	Bottom layer	N.A.	The release profile of TTC, in PBS (pH 7.4), from PP3T5T showed an initial burst release of 47.2% within the first 6 h, followed by a slow release that reached 61.9% until day 4	[25]
					The burst release of TTC, in PBS (pH 7.4), from PPT5T5 was 50.8% within the first 6 h and reached 77% over 4 days	
	PLLA-SS/PLLA	NFZ	Both layers	N.A.	The top PLLA-SS nanofibrous mats with 0.2% of NFZ, in PBS (pH 7.4) presented a fast release profile with more than 98% of NFZ detected in 10 min of incubation for every ratio	[26]
					The PLLA bottom layer in PBS (pH 7.4) presented a more controlled and sustained release, reaching 17.6% after 48 h	
					PLLA-SS(2:1)-0.2NFZ/PLLA-2NFZ, PLLA-	

Aims	Composition	Biomolecule Incorporated	Layer of Incorporation	Encapsulation Efficiency and Loading Efficiency	Release Profile	Ref
					SS(2:1)-0.5NFZ/PLLA-2NFZ, and PLLA-SS(2:1)-1.0NFZ/PLLA-2NFZ in PBS (pH 7.4) presented a burst release of 11.2%, 14.3%, and 28.4%, respectively, and the release amounts reached 29.4%, 43.0%, and 53.9%, respectively, after 48 h	
		Mupirocin	Top layer		The initial burst release of LID reached 66% in the first hours and increased gradually to 85% in the following 6 h, in PBS	
Wound healing improvement	PCL/CS	LID	Bottom layer	N.A.	The release of mupirocin consisted in the release of 57% of mupirocin in the first 6 h, followed by a sustained release (30% was released in the following 114 h), in PBS	[27] [30] [31] [31][32]
	PeCL/Gel	Pio	Bottom layer	Loading efficiency of 56.16 ± 7.45%	The Pio release rapidly reached 40% in day 1 and a long-term release reached 75% in day 14, in PBS (pH 7.4)	[28]
	PLA/PCL	VE	Both layers	N.A.	The asymmetric membrane showed a sustained release of VE over 21 days reaching a maximum of 78%, in PBS	[29] [30] [33][34]

AV: Aloe vera; CRV: Carvacrol; CS: Chitosan; Gel: Gelatin; HA: Hyaluronic acid; LID: Lidocaine hydrochloride; N.A.: Not available; NFZ: Nitrofurazone; PBS: Phosphate-buffered saline; PCL: Polycaprolactone; PDO:

me ratio, les from ers, and molecule olecules' e of non- e of the es in the medium nposition between ure, i.e., espect to on within rophobic

drugs [31][35]. It is worth noticing that hydrophilic drugs usually present faster drug releases (i.e., burst release) due to their high solubility in the release media [31]. Furthermore, changes in the matrix structure can also influence drug release. For example, an increase in the surface area-to-volume ration and porosity of fibrous mats leads to a burst release of the drugs from the nanofibers [36]. Moreover, the development of fibers with a multilayer structure enables a more sustained release, or even the encapsulation of different therapeutic agents in different layers, each one presenting a release profile according to its location in the fiber [37]. Another strategy that has been emerging is the use of stimuli-responsive materials which facilitate the control of the drug release both temporally and spatially [38][39]. Temperature [40], ultrasound [41], light [42], and endogenous changes in the pH value [43], are

Some examples of the polymers that can be exploited to trigger the drug release by PLA: Poly(lactic acid); PLGA: Poly(lactic-*co*-glycolic acid); PEO: Polyethylene oxide; PCL: Poly(ε-caprolactone); PVAc: Polyvinyl acetate; SA: Salicylic acid; SF: Silk fibroin; SS: Sericin; THY: Thymol; VE: Vitamin E derivative; ZN: Zein.

The incorporation of therapeutic or antimicrobial agents can be performed before (e.g., blend, co-axial, and emulsion) or after (e.g., physical adsorption, layer-by-layer assembly, and chemical immobilization) the electrospinning process [44]. In the blend electrospinning, the drug is incorporated in the polymeric solution and the nanofibers are produced with the drug uniformly distributed within their structure [45]. The resulting nanofibrous mats often exhibit a burst release dependent on polymer degradation and drug diffusion from the nanofiber [46]. Alternatively, core-shell nanofibers encapsulate the therapeutic agents within the nanofiber core, which is enclosed in an external polymeric layer that provides a more controlled and prolonged drug release [38]. These nanostructures can be produced by co-axial or by emulsion electrospinning. The co-axial electrospinning uses concentric needles to create a layer-by-layer organization, while the emulsion relies on the utilization of an aqueous solution and an oil phase that are emulsified together to create the core-shell nanofibers [34][35]. Otherwise, the drug loading can be achieved via post-electrospinning techniques that comprise the adsorption of the drug onto the surface of the fibers through non-covalent or covalent interactions [35]. The physical adsorption of therapeutic agents is based on the creation of non-covalent interactions (electrostatic and/or hydrophobic) between the nanofibers and the drug, while the chemical approaches require the immobilization of the therapeutic agents via covalent bonds. Such enables the development of nanofiber membranes with different drug release profiles, i.e., usually non-covalent interactions lead to a faster and poorer control over the drug release, whereas a sustained/stimuli-responsive release can be achieved using covalent binding [46][35]. These different approaches allow the selection of the optimal loading method according to the bioactive agent as well as the possibility to develop wound dressings with tailored release profiles [46]. For example, Buck et al. compared the antimicrobial and release properties of PLGA electrospun fibers incorporating ciprofloxacin (CIP) through blend or physical adsorption [47]. The blend nanofibers were produced by the electrospinning of a CIP-PLGA solution, whereas in the physical adsorption PLGA nanofibrous mats were immersed in a CIP solution and dried. The authors observed that upon the immersion of PLGA mats in phosphate-buffered saline solution (PBS) (pH 7.4), at 37 °C, the CIP loading by physical absorption resulted in a fast release, reaching its maximum at 6 h. In turn, the blend counterparts presented a sustained release for 48 h. Moreover, the authors also reported that the antibacterial capacity against *Pseudomonas aeruginosa* (*P. aeruginosa*), *Staphylococcus aureus* (*S. aureus*), and *S. epidermidis* was influenced by the loading method. In fact, the physical absorption resulted in higher-sized inhibitory halos, whereas the blended disks retained a higher percentage of the inhibitory zone after 48 h of incubation [47]. In turn, Jin and co-workers compared the incorporation of multiple epidermal induction factors (EIF) by coaxial electrospinning and blend electrospinning, in poly(l-lactic acid)-*co*-poly(ε-caprolactone) (PLLCL) and Gel nanofibers (Gel-PLLCL-EIF (coaxial electrospinning) and Gel-PLLCL-EIF (blend electrospinning), respectively) [48]. To accomplish that, core-shell nanofibers were produced by electrospinning a Gel-PLLCL mixture as an outer solution and 5% bovine serum albumin with a concentrated epidermal induction medium (CEIM, composed of epidermal growth factor (EGF), insulin, hydrocortisone, and retinoic acid) as core solution. Alternatively, the Gel-PLLCL-EIF (blend electrospinning) nanofibers were produced through the conventional electrospinning of the Gel-PLLCL-CEIM blend. These authors observed that the Gel-PLLCL-EIF (blend electrospinning) released 44.9% of its content in the first 3 days, reaching

the maximum of 77.8% at day 15, whereas the Gel-PLLCL-EIF (coaxial electrospinning) presented a stable and sustained release with 50.9% of EGF released at day 15. Such differences were attributed to the Gel-PLLCL outer layer in the core-shell nanofibers that acted as a barrier that diminished the initial burst release [48]. Apart from the structural organization, the drug release of the nanofibrous mats could also be controlled by the biodegradation profile of the polymers or using smart materials responsive to different stimuli [49]. For more information regarding the utilization of nanofibrous structures as drug delivery systems the readers are referred to [30][49][50][51].

2.1. Electrospun Asymmetric Membranes with Antibacterial Activity

When the skin integrity is disrupted, the occurrence of infections leads to the deterioration of the granulation tissue, growth factor, and ECM components and, consequently, to the impairment of the wound healing process [49]. These infections can be caused by different bacteria, usually in initial stages the infections occur as a consequence of Gram-positive bacteria, such as *S. aureus* and *Streptococcus pyogenes* (*S. pyogenes*), while in later stages they are originated by Gram-negative bacteria, such as *Escherichia coli* (*E. coli*) and *P. aeruginosa*. In this way, the incorporation of antibiotics (e.g., CIP, gentamicin, and sulfadiazine), nanoparticles (e.g., silver, iron oxide, nitric oxide), and natural products (e.g., honey, essential oils, and CS) in wound dressing has been widely explored to prevent bacterial infections [14][49].

Among the different antibacterial agents, the incorporation of antibiotics in asymmetric electrospun membranes has been one of the most explored approaches [25][26]. Zhao et al. produced an asymmetric poly(l-lactide) (PLLA)-sericin (SS)/PLLA electrospun membrane loaded with nitrofurazone (NFZ) for wound dressing applications [26]. In this process, the NFZ was blended in the PLLA-SS and PLLA solutions before the electrospinning process. The NFZ-loaded PLLA bottom layer was produced over the NFZ-loaded PLLA-SS nanofibrous mats. The PLLA bottom layer presented fibers with an average diameter of 814 nm. In turn, in the PLLA-SS mats, the average diameter of the nanofibers increased from 413 to 1095 nm by changing the PLLA-SS ratio from 4:1 to 1:1. Despite this variation, the asymmetric membranes presented a similar overall porosity ranging from 75.14 ± 5.43% to 78.35 ± 2.38%. The authors observed that the NFZ presented a release profile dependent on the nanofibrous layer. The top PLLA-SS nanofibrous mats presented a fast release profile with more than 98% of NFZ detected in 10 min of incubation, independently of the PLLA-SS ratio. Otherwise, the PLLA bottom layer presented a more controlled and sustained release, reaching the 17.6% after 48 h. Such difference is attributed to the possible interaction of NFZ with SS, a good water-soluble material that allows a faster drug diffusion upon its dissolution in the media. Moreover, the initial burst release of NFZ from the PLLA-SS layer is important for the elimination of bacteria that can be initially present on the wound site, whereas the more sustained release from the PLLA bottom layer can contribute to long-term antibacterial effects. The studies performed on *E. coli* and *Bacillus subtilis* demonstrated the SS intrinsic antibacterial activity, which was enhanced with the NFZ incorporation (larger inhibitory halos). In in vivo studies, the group treated with the NFZ-loaded asymmetric membranes showed a faster wound healing, i.e., 97 and 84% wound size reduction for the NFZ-loaded dual-layer membranes and commercial woven dressing, respectively [26].

Nevertheless, the rise of multidrug-resistant bacteria over the past years has highlighted the necessity to select and study new antibacterial agents. In this way, natural products have been screened to identify alternative antibacterial approaches. Among them, essential oils have been recognized due to their antioxidant, antiviral, anticancer, insecticidal, anti-inflammatory, anti-allergic, and antimicrobial properties [49]. The antibacterial activity of these natural products is mainly attributed to the phenolic compounds, specifically to thymol (THY) and carvacrol (CRV) [20][22]. Miguel et al. produced a silk fibroin (SF)-based asymmetric electrospun membrane loaded with THY for being applied in the wound healing [20]. The THY was blended in a SF-HA solution that was electrospun over the SF-PCL top layer and treated with ethanol vapor to improve the water stability of the SF. The SF-based asymmetric electrospun membrane presented an overall porosity of 74.78 ± 6.98%, a swelling capacity of 400%, and nanofibers with a mean diameter of 615.9 ± 190.4 and 412.7 ± 106.7 nm in the top SF-PCL and bottom SF-HA-THY layers, respectively. Moreover, the authors observed a burst release of THY in the first 8 h, reaching a maximum of 91.87 ± 0.99% at pH 8 (Figure 5). Otherwise, the antibacterial assays performed with and *P. aeruginosa* revealed that the SF-PCL top membrane can avoid the infiltration of both bacteria through the bottom layer with an efficacy almost similar to the conventional filter paper. Further, the SF-HA-THY bottom membrane significantly inhibited the proliferation of *S. aureus* and *P. aeruginosa* (bacterial growth inhibition of 87.42% and 58.43%, respectively) when compared to the SF-HA membrane (4.05% and 3.42%) [20].

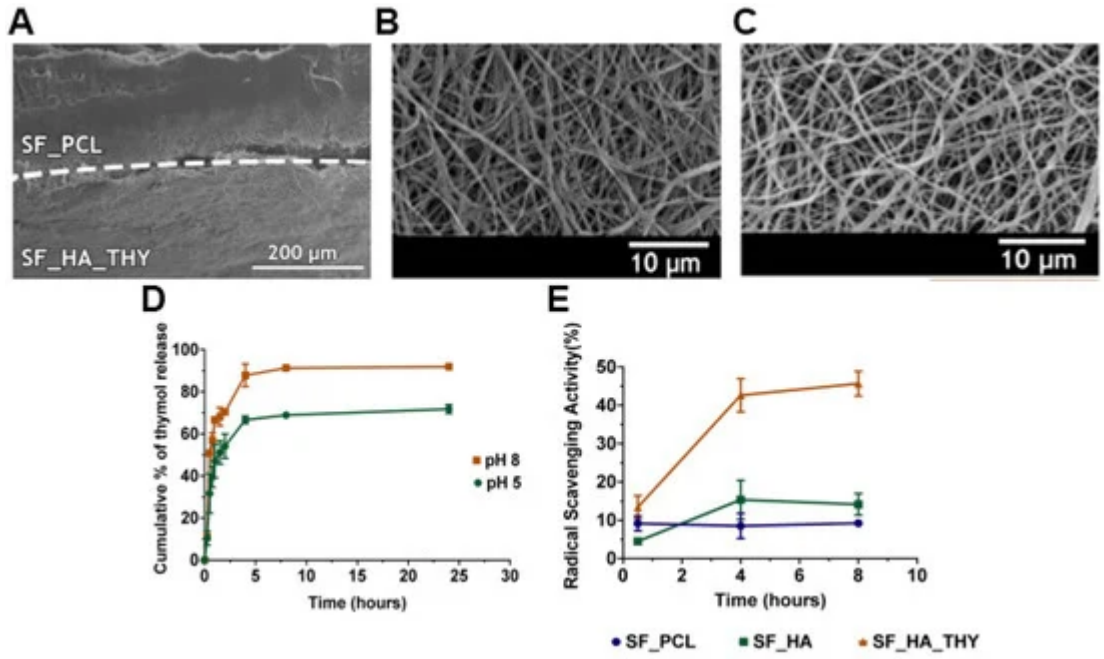

Figure 5. SEM images of (**A**) produced asymmetric membrane cross-section (top layer: SF_PCL; bottom layer: SF_HA_THY); (**B**) SF_PCL after the crosslinking process; (**C**) SF_HA_THY after the crosslinking process; (**D**) evaluation of the THY In Vitro release profile; (**E**) evaluation of the antioxidant activity of the SF-PCL membrane (top layer), SF-HA membrane (bottom layer) with or without THY. Reprinted with permission from [20], Elsevier, 2019.

In a similar approach, Aragón and co-workers produced a PCL/poly(vinyl acetate) (PVAc) asymmetric membrane loaded with CRV for increasing the antimicrobial capacity of the wound dressing [22]. The production of the

asymmetric membrane was accomplished in a three-step process using a multi-jet electrospinning apparatus: 1) Deposition of PCL top layer; 2) multi-jet deposition of PCL and PVAc-CRV blend; and 3) deposition of PVAc-CRV bottom layer. The PCL/PVAc asymmetric membrane presented an overall porosity superior to 80%, comprising a denser hydrophobic PCL top layer with a thickness around 100–120 µm and fibers with an average diameter of 360 ± 68 nm, a transition layer, and a loose spiderweb PVAc-CRV nanofibrous structure with an average diameter of 600 ± 100 nm. Moreover, the CRV release assays performed in conditions mimicking the wound site (pH 8 to 5) showed an initial burst release ≈45% after 24 h, at pH 8, followed by a sustained diffusion up to 85% at day 21 and pH progression from 8 to 7.4 and 5. Moreover, the authors reported that the PCL/PVAc-CRV asymmetric membrane significantly inhibited the proliferation of *E. coli* (from 1.6×10^9 to 1.2×10^7) and *S. aureus* (5.7×10^{10} to 2.3×10^7) [22].

2.2. Electrospun Asymmetric Membranes Loaded with Bioactive Molecules that Improve the Healing Process

The wound healing process involves five different phases, namely hemostasis, inflammation, migration, proliferation, and remodeling. This complex process is based on a complex interaction between cells, growth factors, and cytokines [52]. In this way, tissue engineering researchers have been incorporating bioactive molecules in wound dressings to promote and improve the different phases of the healing process.

The delivery of vitamins can stimulate cell migration to the wound site, increase the collagen synthesis, enhance the angiogenesis, and modulate the inflammatory response leading to an improved skin regeneration [53]. Zahid and collaborators produced a PCL/PLA electrospun membrane enriched with α-tocopherol acetate (vitamin E derivative-VE) for supporting the wound healing process [29]. The VE was blended both with PCL and PLA solutions, then the PLA-VE blend was electrospun over the assembled PCL-VE top layer using a rotating collector. The asymmetric membrane showed a sustained release of VE over 21 days reaching a maximum of 78%. Further, the authors observed that the VE-loaded PCL/PLA asymmetric membrane was capable of promoting the NIH3T3 fibroblasts cell migration, adhesion, and proliferation. Additionally, the studies performed on chick chorioallantoic membrane showed that the group treated with VE-loaded PCL/PLA asymmetric membrane presented a higher number of blood vessels, i.e., 2-times superior to that detected on non-loaded PCL/PLA bilayers (Figure 6).

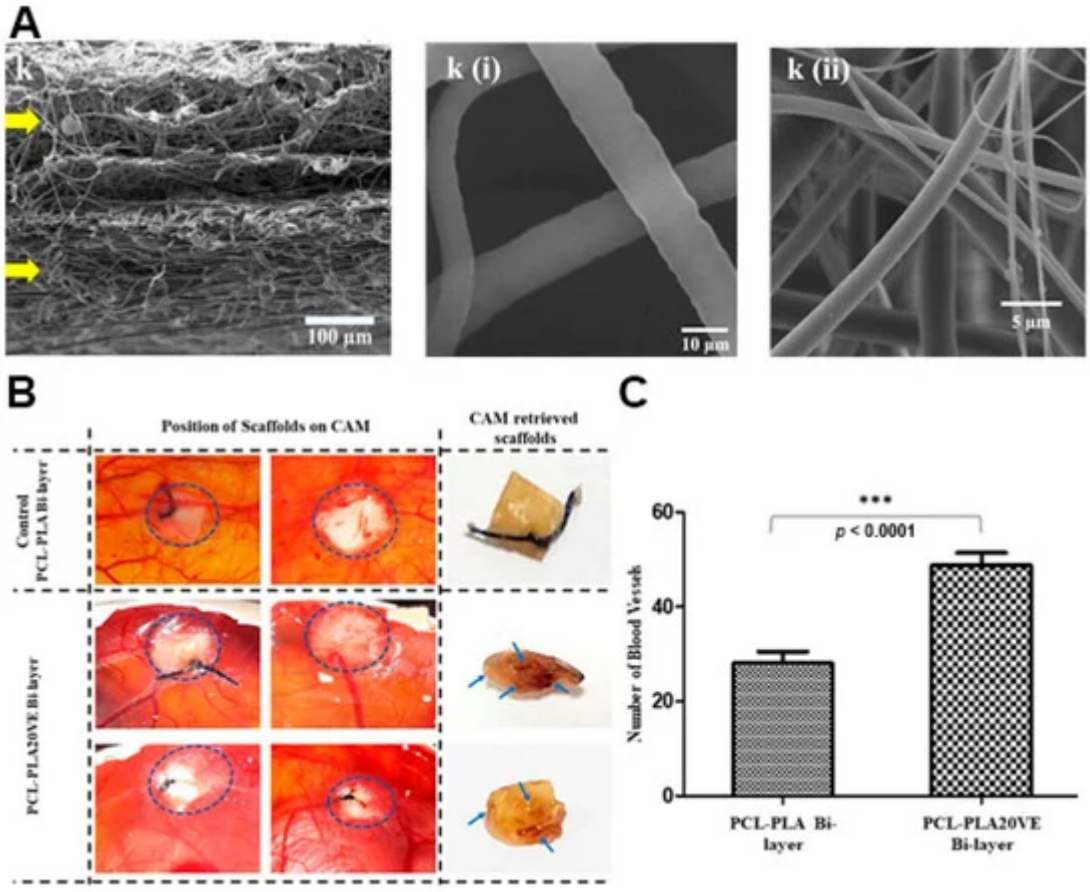

Figure 6. (**A**) SEM images of cross section of PCL-PLA20VE Bi-layer; k(i) PCL20VE; k(ii) PLA20VE. (**B**) Evaluation of angiogenic potential of the PCL/PLA asymmetric membranes with and without 20% of VE. The appearance and position of implanted membranes on CAM, at day 14 of fertilization, indicated by the circles. Blue arrows, on retrieved membranes, depict blood vessels infiltrated inside the explanted membrane. (**C**) Quantification of CAM assay by counting blood vessels around and inside the membranes, from the images taken at day 14, just before retrieving the membranes and sacrificing the eggs. The results are mean ± S.D. (*** $p < 0.0001$) of 4 viable chicks surviving from original group of 7 fertilized eggs per group. Reprinted with permission from [29], Elsevier, 2019.

Otherwise, the asymmetric membranes can also be loaded with anti-inflammatory agents, such as curcumin, chrysin, ibuprofen, and pioglitazone (Pio) [14][28][54]. A chronic or uncontrolled acute inflammatory process could result in excessive production of inflammatory mediators, free radicals, and cytotoxic enzymes that could negatively impact on the healing process [49]. Yu et al. developed a poly(ε-caprolactone) (PeCL)/Gel nanofibrous asymmetric membrane loaded with Pio using a 40 µm-pore-size nylon mesh template [28]. The hydrophobic PeCL layer was electrospun on the top side of the nylon mesh template, whereas the hydrophilic Gel-Pio blend was produced on the bottom side and crosslinked with genipin. The resulting membrane is composed of 270 nm diameter PeCL nanofibers on top and 144 nm Gel nanofibers in the bottom layer. The Pio release from the PeCL/Gel asymmetric membrane rapidly reaches 40% in day 1 and stabilizes around 75% until day 14. Bacterial adhesion tests performed with *S. aureus*, *P. aeruginosa*, and *E. coli* demonstrated that the PeCL top layer significantly reduced the number of adhered bacteria, particularly for *P. aeruginosa* and *E. coli* strains, due to its

hydrophobicity (surface water contact angle of 145°). Furthermore, when compared to the non-loaded counterparts, the PeCL/Gel-Pio asymmetric membranes promoted the migration of both human skin fibroblasts and human umbilical vein endothelial cells. Moreover, the authors also observed a clear reticular vascular structure with more tube junctions and nodes in the HUVECs group treated with PeCL/Gel-Pio demonstrating its proangiogenic capacity. The in vivo assays performed on type 2 diabetic mice showed that the wounds treated with the PeCL/Gel-Pio asymmetric membrane were almost fully closed on day 10, whereas the same was only observed at day 14 in the groups treated with PeCL/Gel and Tegaderm. Further, at day 14, the PeCL/Gel-Pio group presented a relative collagen content almost 2-times superior to the remaining groups, being also observed in histological images' regular and orderly collagen arrangement as well as a smaller granulation tissue space [28].

References

1. Guerra, A.; Belinha, J.; Jorge, R.N. Modelling skin wound healing angiogenesis: A review. J. Theor. Biol. 2018, 459, 1–17.
2. Wong, R.; Geyer, S.; Weninger, W.; Guimberteau, J.-C.; Wong, J.K.F. The dynamic anatomy and patterning of skin. Exp. Dermatol. 2016, 25, 92–98.
3. Ghomi, E.R.; Khalili, S.; Khorasani, S.N.; Neisiany, R.E.; Ramakrishna, S. Wound dressings: Current advances and future directions. J. Appl. Polym. Sci. 2019, 136, 47738.
4. Pereira, R.F.; Bartolo, P.J. Traditional therapies for skin wound healing. Adv. Wound Care 2016, 5, 208–229.
5. Dixit, S.; Baganizi, D.R.; Sahu, R.; Dosunmu, E.; A Chaudhari, A.; Vig, K.; Pillai, S.R.; Singh, S.R.; Dennis, V. Immunological challenges associated with artificial skin grafts: Available solutions and stem cells in future design of synthetic skin. J. Biol. Eng. 2017, 11, 49.
6. Dreifke, M.B.; Jayasuriya, A.A.; Jayasuriya, A.C. Current wound healing procedures and potential care. Mater. Sci. Eng. C 2015, 48, 651–662.
7. Haddad, A.G.; Giatsidis, G.; Orgill, D.P.; Halvorson, E.G. Skin substitutes and bioscaffolds: Temporary and permanent coverage. Clin. Plast. Surg. 2017, 44, 627–634.
8. Aljghami, M.E.; Saboor, S.; Amini-Nik, S. Emerging innovative wound dressings. Ann. Biomed. Eng. 2019, 47, 659–675.
9. In, S.M.; An, H.G.; Kim, J.-Y.; Lee, K.-I. Columellar Wound Immediately After Open Rhinoseptoplasty Treated With Application of DuoDERM Extra Thin. J. Craniofacial Surg. 2020, 32, e98.
10. Alinejad, F.; Momeni, M.; Fatemi, M.J.; Dahmardehei, M.; Naderi, S.; Akhoondinasab, M.R.; Zayedly, M.; Mahboubi, O.; Rahbar, H. Comparing the effect of two types of silver nano-crystalline

dressings (acticoat and agcoat) in the treatment of full thickness burn wound. Iran. J. Microbiol. 2018, 10, 378.

11. Kuo, F.-C.; Chen, B.; Lee, M.S.; Yen, S.-H.; Wang, J.-W. AQUACEL® Ag surgical dressing reduces surgical site infection and improves patient satisfaction in minimally invasive total knee arthroplasty: A prospective, randomized, controlled study. Biomed Res. Int. 2017, 2017, 1262108.
12. Chen, S.; Huan, Z.; Zhang, L.; Chang, J. The clinical application of a silicate-based wound dressing (DermFactor®) for wound healing after anal surgery: A randomized study. Int. J. Surg. 2018, 52, 229–232.
13. Kim, H.; Makin, I.; Skiba, J.; Ho, A.; Housler, G.; Stojadinovic, A.; Izadjoo, M. Antibacterial efficacy testing of a bioelectric wound dressing against clinical wound pathogens. Open Microbiol. J. 2014, 8, 15.
14. Simões, D.; Miguel, S.P.; Ribeiro, M.P.; Coutinho, P.; Mendonça, A.G.; Correia, I.J. European Journal of Pharmaceutics and Biopharmaceutics Recent advances on antimicrobial wound dressing: A review. Eur. J. Pharm. Biopharm. 2018, 127, 130–141.
15. Dias, J.; Granja, P.; Bártolo, P. Advances in electrospun skin substitutes. Prog. Mater. Sci. 2016, 84, 314–334.
16. Goodarzi, P.; Falahzadeh, K.; Nematizadeh, M.; Farazandeh, P.; Payab, M.; Larijani, B.; Beik, A.T.; Arjmand, B. Tissue engineered skin substitutes. In Cell Biology and Translational Medicine; Springer: Berlin/Heidelberg, Germany, 2018; Volume 3, pp. 143–188.
17. Pan, C. Gas separation by permeators with high-flux asymmetric membranes. Aiche J. 1983, 29, 545–552.
18. Opong, W.S.; Zydney, A.L. Diffusive and convective protein transport through asymmetric membranes. Aiche J. 1991, 37, 1497–1510.
19. Zhang, D.; Patel, P.; Strauss, D.; Qian, X.; Wickramasinghe, S.R. Modeling tangential flow filtration using reverse asymmetric membranes for bioreactor harvesting. Biotechnol. Prog. 2020, e3084.
20. Miguel, S.P.; Simões, D.; Moreira, A.F.; Sequeira, R.S.; Correia, I.J. Production and characterization of electrospun silk fibroin based asymmetric membranes for wound dressing applications. Int. J. Biol. Macromol. 2019, 121, 524–535.
21. Norouzi, M.; Boroujeni, S.M.; Omidvarkordshouli, N.; Soleimani, M. Advances in skin regeneration: Application of electrospun scaffolds. Adv. Healthc. Mater. 2015, 4, 1114–1133.
22. Aragón, J.; Costa, C.; Coelhoso, I.; Mendoza, G.; Aguiar-Ricardo, A.; Irusta, S. Electrospun asymmetric membranes for wound dressing applications. Mater. Sci. Eng. C 2019, 103, 109822.

23. Figueira, D.R.; Miguel, S.P.; De Sá, K.D.; Correia, I.J. Production and characterization of polycaprolactone-hyaluronic acid/chitosan-zein electrospun bilayer nanofibrous membrane for tissue regeneration. Int. J. Biol. Macromol. 2016, 93, 1100–1110.
24. Miguel, S.P.; Ribeiro, M.P.; Coutinho, P.; Correia, I.J. Electrospun polycaprolactone/aloe vera_chitosan nanofibrous asymmetric membranes aimed for wound healing applications. Polymers 2017, 9, 183.
25. Rezk, A.I.; Lee, J.Y.; Son, B.C.; Park, C.H.; Kim, C.S. Bi-layered Nanofibers Membrane Loaded with Titanium Oxide and Tetracycline as Controlled Drug Delivery System for Wound Dressing Applications. Polymers 2019, 11, 1602.
26. Zhao, R.; Li, X.; Sun, B.; Tong, Y.; Jiang, Z.; Wang, C. Nitrofurazone-loaded electrospun PLLA/sericin-based dual-layer fiber mats for wound dressing applications. RSC Adv. 2015, 5, 16940–16949.
27. Li, X.; Wang, C.; Yang, S.; Liu, P.; Zhang, B. Electrospun PCL/mupirocin and chitosan/lidocaine hydrochloride multifunctional double layer nanofibrous scaffolds for wound dressing applications. Int. J. Nanomed. 2018, 13, 5287.
28. Yu, B.; He, C.; Wang, W.; Ren, Y.; Yang, J.; Guo, S.; Zheng, Y.; Shi, X. Asymmetric Wettable Composite Wound Dressing Prepared by Electrospinning with Bioinspired Micropatterning Enhances Diabetic Wound Healing. ACS Appl. Bio Mater. 2020, 3, 5383–5394.
29. Zahid, S.; Khalid, H.; Ikram, F.; Iqbal, H.; Samie, M.; Shahzadi, L.; Shah, A.T.; Yar, M.; Chaudhry, A.A.; Awan, S.J.; et al. Bi-layered α-tocopherol acetate loaded membranes for potential wound healing and skin regeneration. Mater. Sci. Eng. C 2019, 101, 438–447.
30. Balusamy, B.; Celebioglu, A.; Senthamizhan, A.; Uyar, T. Progress in the design and development of “fast-dissolving” electrospun nanofibers based drug delivery systems-A systematic review. J. Control. Release 2020, 326, 482–509.
31. Zhang, Q.; Li, Y.; Lin, Z.Y.; Wong, K.K.Y.; Lin, M.; Yildirimer, L.; Zhao, X. Electrospun polymeric micro/nanofibrous scaffolds for long-term drug release and their biomedical applications. Drug Discov. Today 2017, 22, 1351–1366.
32. Yang, G.; Li, X.; He, Y.; Ma, J.; Ni, G.; Zhou, S. From nano to micro to macro: Electrospun hierarchically structured polymeric fibers for biomedical applications. Prog. Polym. Sci. 2018, 81, 80–113.
33. Khalf, A.; Madihally, S.V. Recent advances in multiaxial electrospinning for drug delivery. Eur. J. Pharm. Biopharm. 2017, 112, 1–17.
34. Cheng, H.; Yang, X.; Che, X.; Yang, M.; Zhai, G. Biomedical application and controlled drug release of electrospun fibrous materials. Mater. Sci. Eng. C 2018, 90, 750–763.

35. Kamble, P.; Sadarani, B.; Majumdar, A.; Bhullar, S. Nanofiber based drug delivery systems for skin: A promising therapeutic approach. J. Drug Deliv. Sci. Technol. 2017, 41, 124–133.
36. Wang, W.; Zhou, S.; Liu, Z.; Yang, W.; Lin, Y.; Qian, H.; Gao, F.; Li, G. Investigation on the structural properties of GaN films grown on La0. 3Sr1. 7AlTaO6 substrates. Mater. Res. Express 2014, 1, 025903.
37. Jeckson, T.A.; Neo, Y.P.; Sisinthy, S.P.; Gorain, B. Delivery of therapeutics from layer-by-layer electrospun nanofiber matrix for wound healing: An update. J. Pharm. Sci. 2020, 110, 635–653.
38. Chen, S.; Li, R.; Li, X.; Xie, J. Electrospinning: An enabling nanotechnology platform for drug delivery and regenerative medicine. Adv. Drug Deliv. Rev. 2018, 132, 188–213.
39. Pant, B.; Park, M.; Park, S.-J. Drug delivery applications of core-sheath nanofibers prepared by coaxial electrospinning: A review. Pharmaceutics 2019, 11, 305.
40. Li, L.; Yang, G.; Zhou, G.; Yi, W.; Zheng, X.; Zhou, S. Thermally switched release from a Nanogel-in-microfiber device. Adv. Healthc. Mater. 2015, 4, 1658–1663.
41. Yohe, S.T.; Kopechek, J.A.; Porter, T.M.; Colson, Y.L.; Grinstaff, M. Triggered drug release from Superhydrophobic meshes using high-intensity focused ultrasound. Adv. Healthc. Mater. 2013, 2, 1204–1208.
42. Sun, J.; Song, L.; Fan, Y.; Tian, L.; Luan, S.; Niu, S.; Ren, L.; Ming, W.; Zhao, J. Synergistic photodynamic and photothermal antibacterial nanocomposite membrane triggered by single NIR light source. ACS Appl. Mater. Interfaces 2019, 11, 26581–26589.
43. Miguel, S.P.; Ribeiro, M.P.; Brancal, H.; Coutinho, P.; Correia, I.J. Thermoresponsive chitosan–agarose hydrogel for skin regeneration. Carbohydr. Polym. 2014, 111, 366–373.
44. Miguel, S.P.; Figueira, D.R.; Simões, D.; Ribeiro, M.P.; Coutinho, P.; Ferreira, P.; Correia, I.J. Electrospun polymeric nanofibres as wound dressings: A review. Colloids Surf. B Biointerfaces 2018, 169, 60–71.
45. Aavani, F.; Khorshidi, S.; Karkhaneh, A. A concise review on drug-loaded electrospun nanofibres as promising wound dressings. J. Med. Eng. Technol. 2019, 43, 38–47.
46. Wang, J.; Windbergs, M. Functional electrospun fibers for the treatment of human skin wounds. Eur. J. Pharm. Biopharm. 2017, 119, 283–299.
47. Buck, E.; Maisuria, V.; Tufenkji, N.; Cerruti, M. Antibacterial Properties of PLGA Electrospun Scaffolds Containing Ciprofloxacin Incorporated by Blending or Physisorption. Acs Appl. Bio Mater. 2018, 1, 627–635.
48. Jin, G.; Prabhakaran, M.P.; Kai, D.; Ramakrishna, S. Controlled release of multiple epidermal induction factors through core–shell nanofibers for skin regeneration. Eur. J. Pharm. Biopharm. 2013, 85, 689–698.

49. Miguel, S.P.; Sequeira, R.S.; Moreira, A.F.; Cabral, C.S.; Mendonça, A.G.; Ferreira, P.; Correia, I.J. An overview of electrospun membranes loaded with bioactive molecules for improving the wound healing process. Eur. J. Pharm. Biopharm. 2019, 139, 1–22.
50. Thakkar, S.; Misra, M. Electrospun polymeric nanofibers: New horizons in drug delivery. Eur. J. Pharm. Sci. 2017, 107, 148–167.
51. Hu, X.; Liu, S.; Zhou, G.; Huang, Y.; Xie, Z.; Jing, X. Electrospinning of polymeric nanofibers for drug delivery applications. J. Control. Release 2014, 185, 12–21.
52. Boateng, J.S.; Matthews, K.H.; Stevens, H.N.; Eccleston, G.M. Wound healing dressings and drug delivery systems: A review. J. Pharm. Sci. 2008, 97, 2892–2923.
53. Palmieri, B.; Vadalà, M.; Laurino, C. Nutrition in wound healing: Investigation of the molecular mechanisms, a narrative review. J. Wound Care 2019, 28, 683–693.
54. Ranjith, R.; Balraj, S.; Ganesh, J.; Milton, M.J. Therapeutic agents loaded chitosan-based nanofibrous mats as potential wound dressings: A review. Mater. Today Chem. 2019, 12, 386–395.